N92-21943

Millimeter and Hard X-ray/γ–ray Observations of Solar Flares During the June 91 GRO Campaign

M. R. Kundu, S. M. White, N. Gopalswamy and J. Lim

Dept. of Astronomy, Univ. of Maryland, College Park MD 20742

Introduction

The millimeter region has perhaps been the most under-utilized observing wavelength range in solar physics, due to the lack of telescopes which can match the temporal and spatial resolution available at other wavelengths. The usefulness of millimeter-wave observations lies in the fact that they are sensitive to both the highest energy electrons in flares as well as to cool material in the chromosphere. Most millimeter-wave observations of solar flares have been hampered both by poor spatial resolution (because of the lack of synthesis interferometers) and by poor sensitivity (since the flux from the Sun's thermal emission is so high at millimeter wavelengths). The number of reported observations of bursts at millimeter wavelengths is relatively small, and there are none for which true high-spatial-resolution imaging data have been reported (see review by White and Kundu 1992).

The emission of solar flares at millimeter wavelengths is of great interest both in its own right and because it is generated by the very energetic electrons which also emit gamma rays. Since high-resolution imaging at gamma-ray energies is not presently possible, millimeter observations can act as a substitute. In addition, the millimetric emission is undoubtedly optically thin (except possibly for a small class of very large flares which have spectra rising beyond 100 GHz; Kaufmann *et al.* 1985), and thus is not subject to the same ambiguities of interpretation which are prevalent in the study of solar microwave bursts. It can be used as a powerful diagnostic of the energy distribution of electrons in solar flares and its evolution, and of the magnetic field.

We have carried out high-spatial-resolution millimeter observations of solar flares using the Berkeley-Illinois-Maryland Array (BIMA). At the present time BIMA consists of only three elements, which is not adequate for mapping highly variable solar phenomena, but is excellent for studies of the temporal structure of flares at millimeter wavelengths at several different spatial scales. The first dedicated observations of solar flares with a high-spatial-resolution millimeter-wavelength interferometer were made by us in March 1989 (Kundu *et al.* 1990) when a solar active region with the greatest X-ray flare production rate yet recorded appeared on the disk of the Sun. Our observations represented an improvement of an order of magnitude in both sensitivity and spatial resolution compared with previous solar observations at these wavelengths. We found that most of the flares occurring within the field of view during the March '89 observations were detected at millimeter wavelengths, including both very impulsive

and longer-duration events. Of 18 flares listed by SGD during our observations, BIMA detected 14, including all those with GOES X-ray classes of C or greater (3 X-class, 7 M-class and 2 C-class). The four flares which BIMA did not detect were all of optical class SF and undetected in X-rays. For 3 of the 4, no microwave emission was reported. Thus only in one flare was microwave emission reported without a detection at BIMA. On the other hand, there were 3 flares for which BIMA detected emission but no events were reported by microwave patrols.

Based on those early observations it appeared that millimeter burst sources were not much smaller than microwave sources; generally source sizes were in excess of 2″, but in some events sources may be $\sim 1″$. Thermal gyrosynchrotron models for the radio emission in the impulsive phase could be ruled out because the flux at millimeter wavelengths was too high.

In this paper, we present BIMA observations made during the GRO/Solar Max '91 Campaign in June 1991 when solar activity was unusually high. Our observations covered the period June 8 – June 13, 1991; this period overlapped the period June 4–June 15 when the Compton Telescope made the Sun a target of opportunity because of the high level of solar activity.

Observations

During the period of June 8–13, 1991, BIMA was in its most compact configuration. The array presently has three antennas, providing three baselines. In effect each baseline provides a one–dimensional spatial Fourier transform of the brightness distribution on the sky. For a point source the phase gives us positional information, while the amplitude is the total flux of the source. For an extended source the response of the interferometer depends on the relationship of the source dimension to the fringe spacing of the Fourier transform: only if the source dimension is smaller than about one-third of the fringe spacing do we expect the amplitude variability to correspond to the total flux in the source. For the 1991 June observations the fringe spacing ranged from $\sim 30″$ EW to $\sim 45″$ NS; such large fringe spacings should guarantee that the correlated amplitude corresponds to the total flux of the source, at the expense of information about small spatial scales. To summarize the properties of millimeter-wavelength emission from solar flares, in Figure 1 we show the correlated amplitude on a single baseline (31) for the whole period of observation with the BIMA array in 1991 June. Most of the larger events can be seen (about 30 radio bursts in total were detected by BIMA and some of the smaller ones do not show up well on this plot). Two timescales of emission are readily seen in this figure: a rapid rise and fall component which appears as sharp spikes, and a much less rapidly varying component which often follows an impulsive spike. As we discuss further below, and as has long been expected, the impulsive component corresponds to nonthermal gyrosynchrotron emission from energetic electrons, while the long-duration events are produced by thermal bremsstrahlung in the hot dense plasma seen in the corona in the decay phase of solar flares. Two of the giant flares from the June period (early UT on June 9 and 11, here shown at the end of June 8 and 10) saturated the telescope receivers shortly after flare onset, and we will not discuss them here.
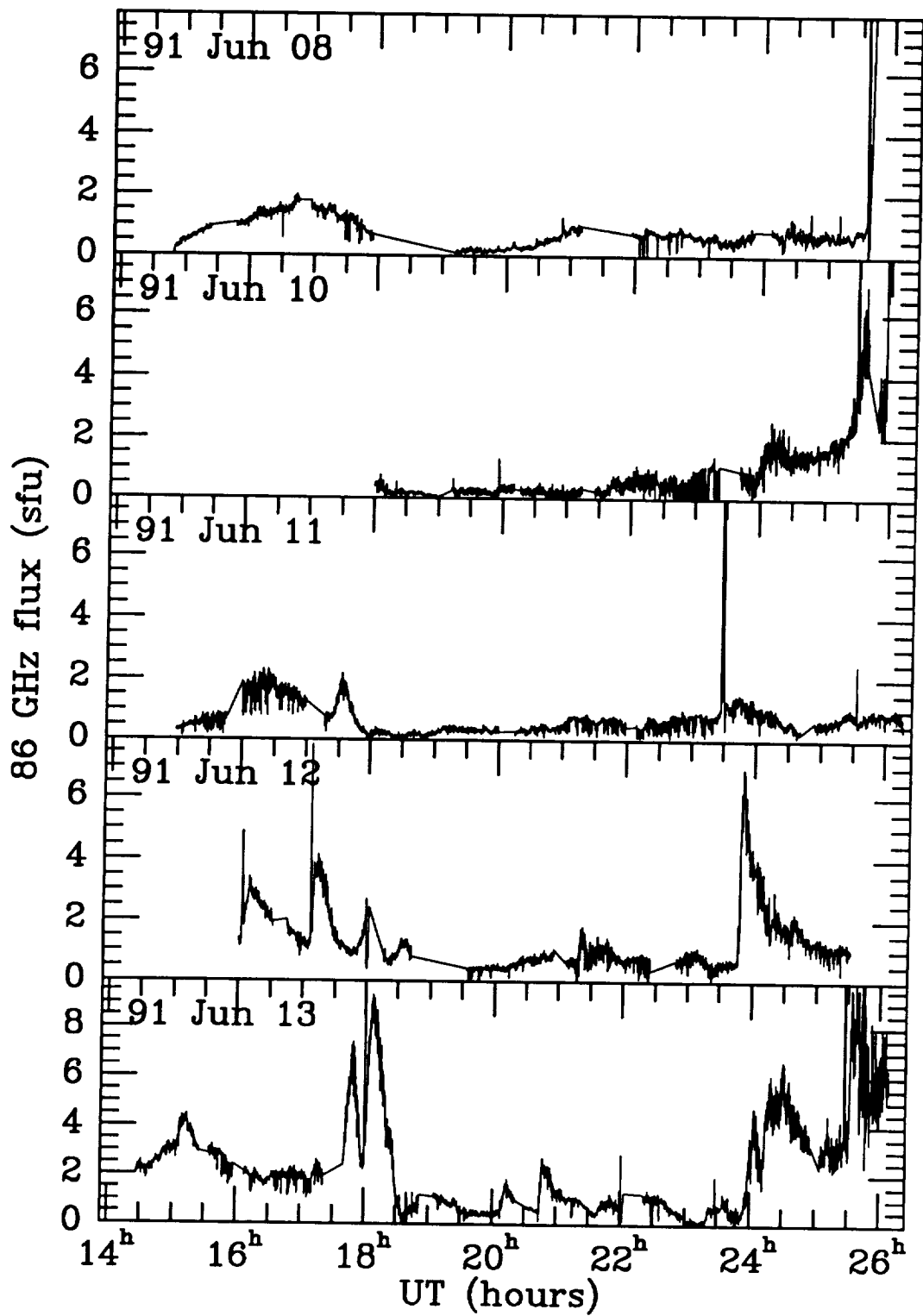
Figure 1 A plot of amplitude versus time (UT hours) summarizing the BIMA 86 GHz observations during the 1991 June GRO solar campaign.
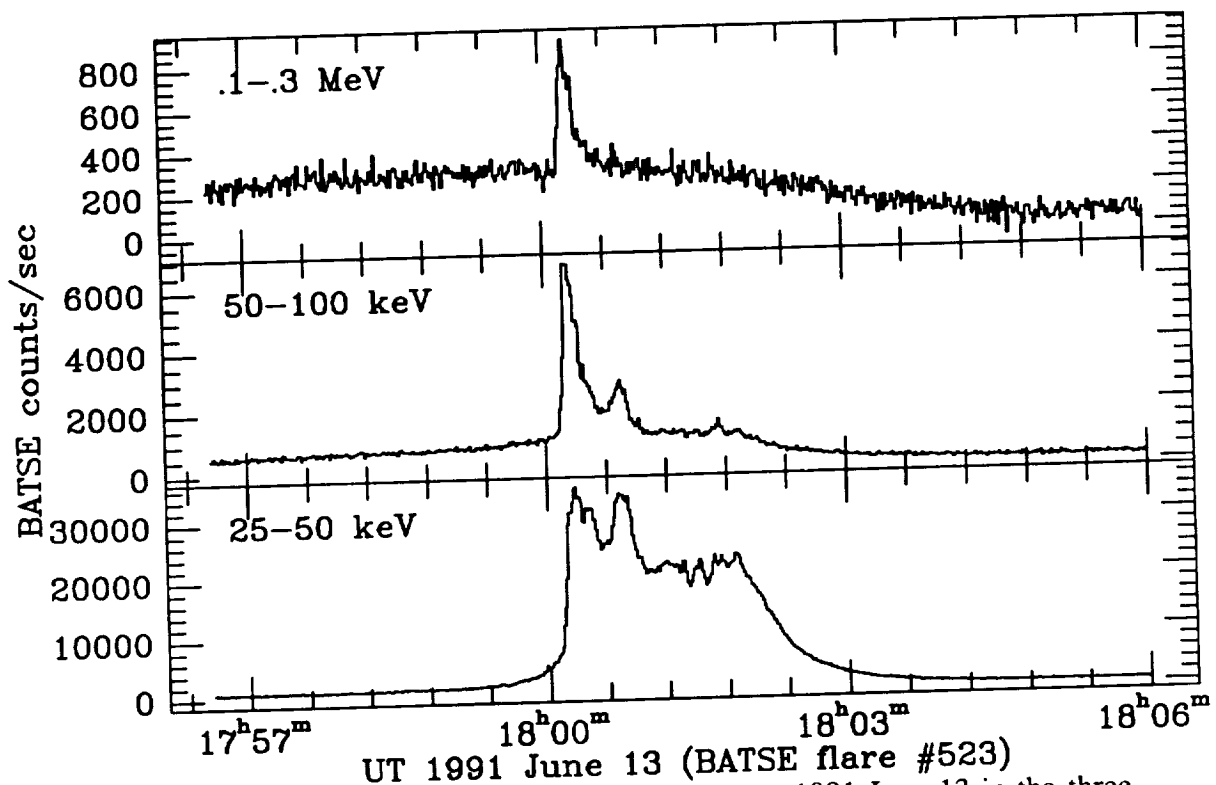
Figure 2 The time profile of a flare observed on 1991 June 13 in the three lowest energy ranges of the BATSE large-area detectors (as labelled). Note that the 25 – 50 keV emission continues much longer than do the higher-energy X-rays: the latter are confined to a hard spike at the onset of the flare. The time resolution of the BATSE data is 1.024 s.

Since we have not completed the analysis of these events along with other data obtained simultaneously, here we shall restrict ourselves to a morphological description of BIMA 86 GHz burst observations and comparison with GRO-BATSE gamma ray burst observations as well as GOES soft X-ray data. Where possible we will demonstrate the scientific results from this type of observation: these arise primarily from the fact that millimeter-wavelength emission is due to the same electrons which emit gamma rays, which we will demonstrate in the first event discussed.

Results

Figure 2 presents the BATSE data for a burst observed on June 13, 1991, ∼ 17:57–18:06 UT. The flare evolution is shown for 3 different energy channels (25–50 keV, 50–100 keV, and 0.1–0.3 MeV; there were no significant counts above the background in the 0.3 – 1 MeV channel). The remarkable feature of this flare is that while the overall profile in the 25 – 50 keV range is relatively unremarkable, with a sharp rise to a plateau level containing a number of sub-peaks followed by a rapid decay, in the higher-energy channels we see a sharp spike right
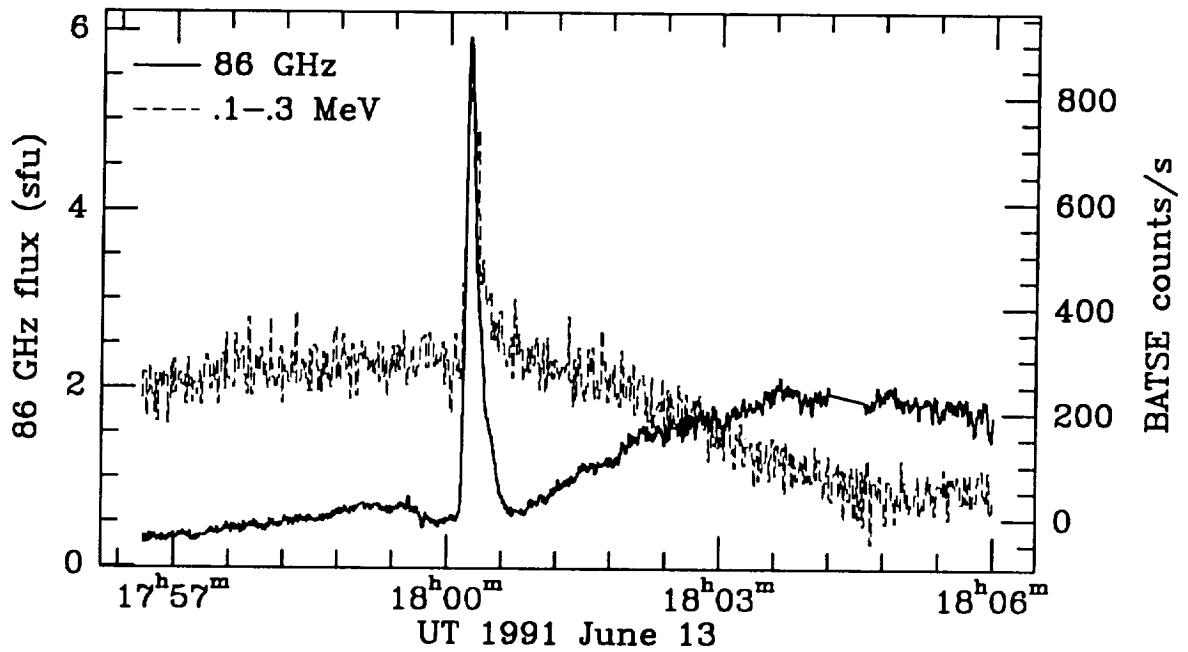
505

Figure 3 Comparison of the time profiles of the 1991 June 13 18 UT flare emission in the 100 – 300 keV hard X-rays seen by BATSE (broken line) and the 86 GHz emission recorded by BIMA (solid line).
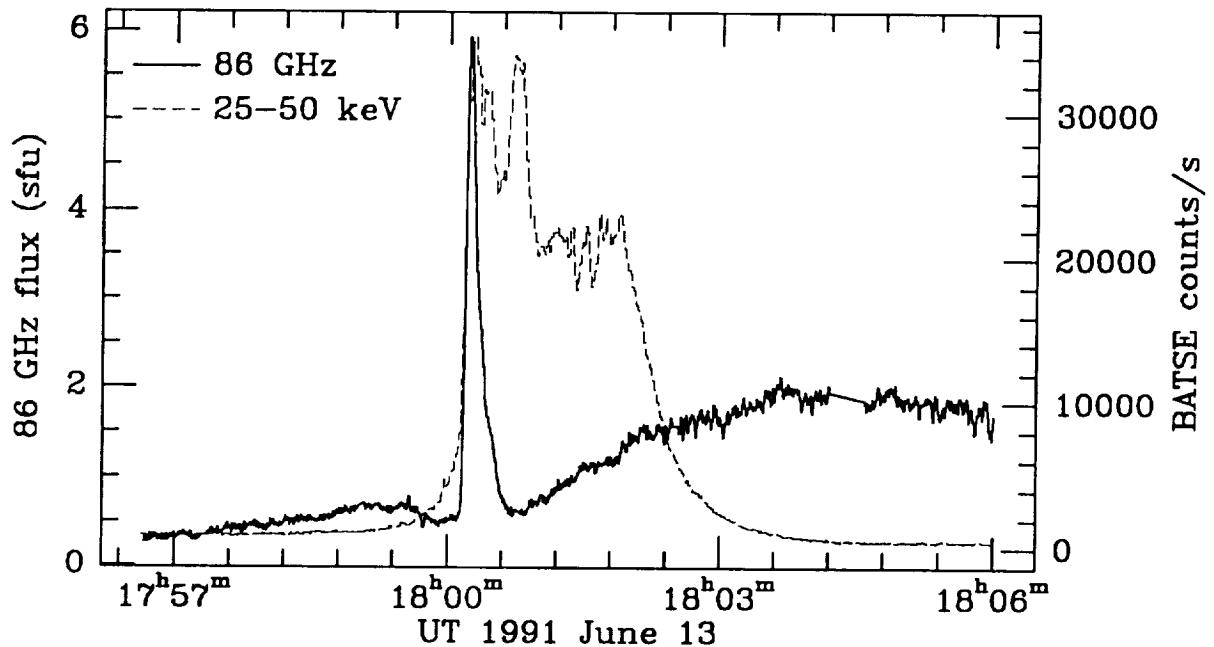

Figure 4 Comparison of the time profiles of the 1991 June 13 18 UT flare emission in 25 – 50 keV hard X-rays and the 86 GHz.

at the beginning of the flare. We and others have argued elsewhere (Ramaty 1969; Ramaty
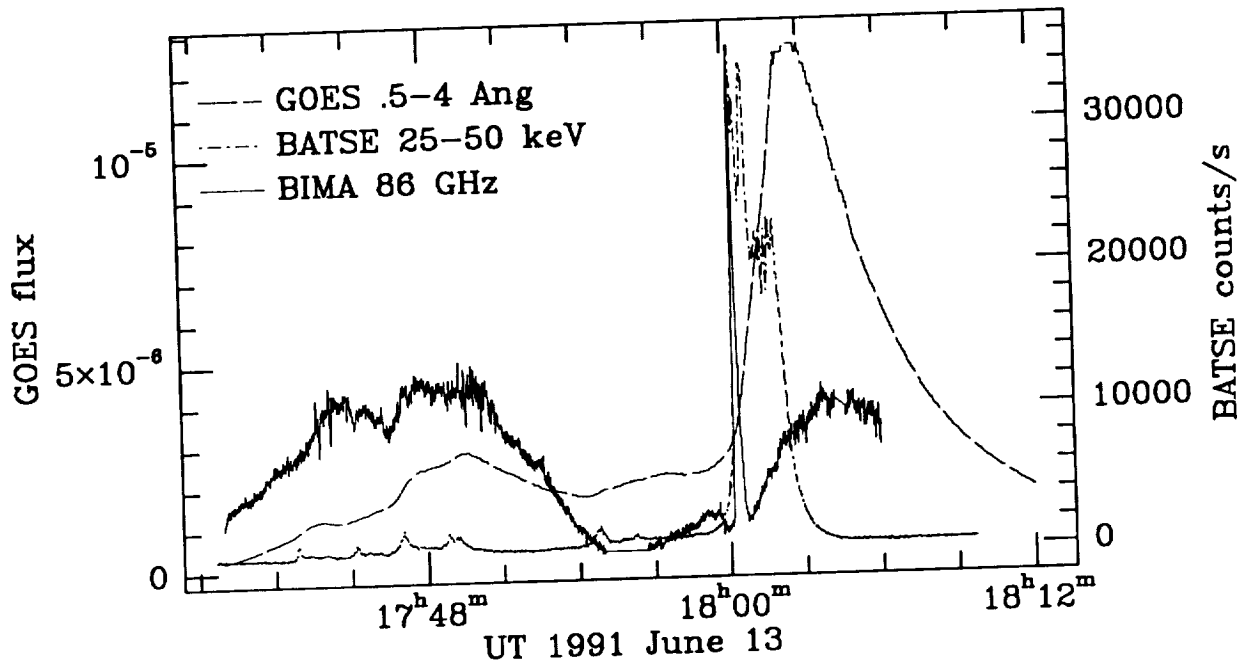
Figure 5 The evolution of emission around 18 UT on 1991 June 13 seen in soft X-rays recorded by the GOES satellite (3 – 25 keV; long-dashed line), in 25 – 50 keV X-rays detected by BATSE (short-dashed line), and at 86 GHz recorded by BIMA (solid line).

& Petrosian 1972; Kundu *et al.* 1990; White & Kundu 1992) that millimeter emission in the impulsive phase should be due to gyrosynchrotron emission from the most energetic electrons in a flare, and on this basis one would predict that the millimeter emission would also show a sharp spike in the onset phase. This is exactly what is seen. In Figure 3 we have plotted the BATSE 0.1–0.3 MeV time profile and the BIMA 86 GHz profile to the same scale. The BATSE data have a time resolution of 1.024 s, while the BIMA data have a time resolution of 0.4 s. The close similarity of the two profiles provides convincing evidence that the millimeter emission is indeed due to the most energetic electrons in a solar flare: the same energetic electrons that produce gamma ray continuum. The importance of this result is that we can obtain high-spatial-resolution information on source structures with millimeter-interferometer observations, which is not presently possible directly with gamma-ray observations.

To emphasize the point, in Figure 4 we compare the BIMA 86 GHz profile with the BATSE 25–50 keV time profile. We see that the sharp rise in the 25–50 keV range coincides exactly with the 86 GHz rise, although there is some emission in the 25 – 50 keV range just prior to the impulsive rise which has no signature at 86 GHz. However, unlike the 25 – 50 keV burst which has a plateau lasting ~ 3 min and contains another major peak, the mm emission drops abruptly to almost its pre-burst emission. This figure also emphasizes that, in addition to the impulsive phase coinciding with the gamma ray emission, the millimeter emission shows an extended component which rises slowly and continues beyond 1806 UT. Thus in this event we clearly see two easily-distinguishable components in the millimeter
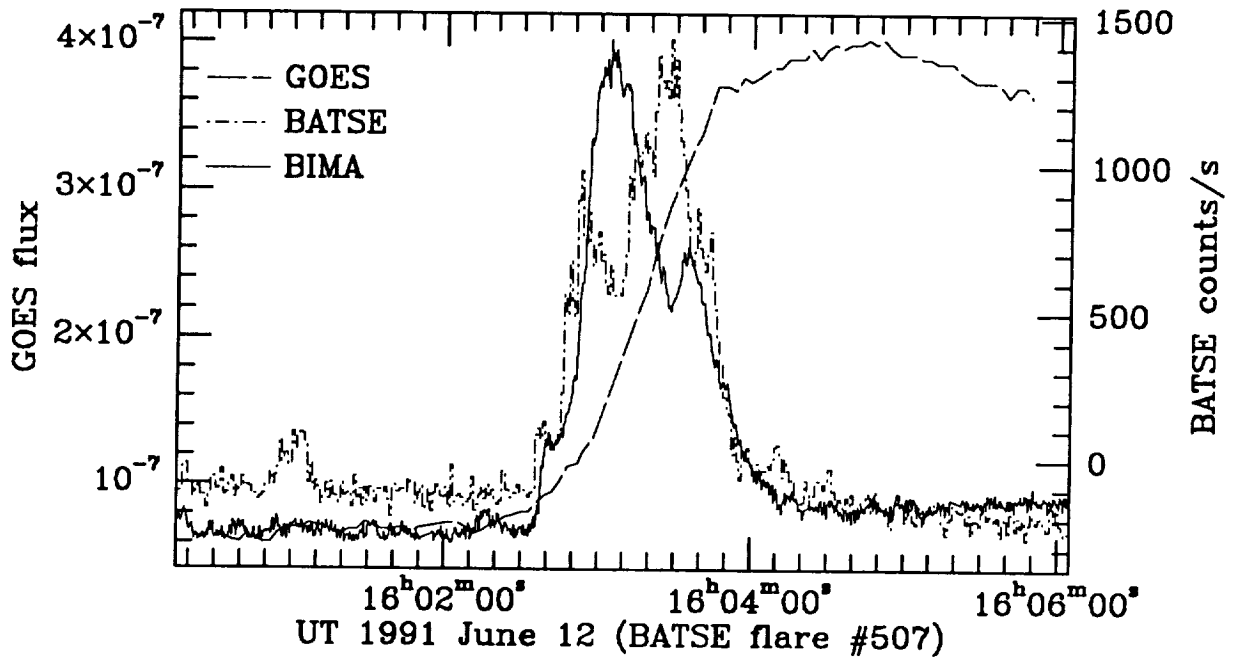
507

Figure 6 The soft X-ray, hard X-ray and 86 GHz time profiles of a flare at 16 UT on June 12.

emission: an impulsive component coinciding in time with the impulsive gamma ray emission, and a gradual extended component with no gamma ray counterpart. We also note the small dip in the 86 GHz emission immediately prior to the impulsive rise, which seems to be a common feature of pre-flare activity in millimeter-wave emission.

Figure 5 shows the complete June 13 event starting at $\sim$ 1736 UT as seen by the GOES satellite soft-X-ray detectors (0.5 - 4 Å, which corresponds to an energy range of 3 - 25 keV; 3 s time resolution), the GRO/BATSE 25–50 keV detectors and BIMA 86 GHz interferometer. This figure has a number of interesting features. The soft X-ray data characteristically show only very smooth variations in time, quite unlike the adjacent 25 - 50 keV time profile, and this is assumed to be because the GOES rates are dominated by low-energy (3 - 10 keV) soft X-rays which are produced by thermal plasma, as opposed to the nonthermal electrons which produce the 25 - 50 keV emission. Prior to the impulsive rise at 18 UT the 86 GHz emission shows a long-duration, slowly-varying emission at quite a high level; the GOES records also show emission at this time, and we attribute both to thermal plasma. In the BATSE profile we see a number of small impulsive peaks between 1736 and 1757 UT, which may be associated with the production of the thermal plasma. It is conceivable that both the BIMA 86 GHz emission and GOES soft X-ray emissions are manifestations of preflare activity. At 18 UT we see the impulsive phase of the main flare in the hard X-rays and at 86 GHz, as already discussed; the soft X-rays show the usual slow rise and fall, with a peak occurring well after the hard-X-ray peak. In the decay phase we also see that the thermal phase at 86 GHz matches the soft-X-ray profile quite well, confirming the interpretation that the long-duration millimeter emission in the decay phase is thermal and associated with the hot dense loops seen in soft X-rays.
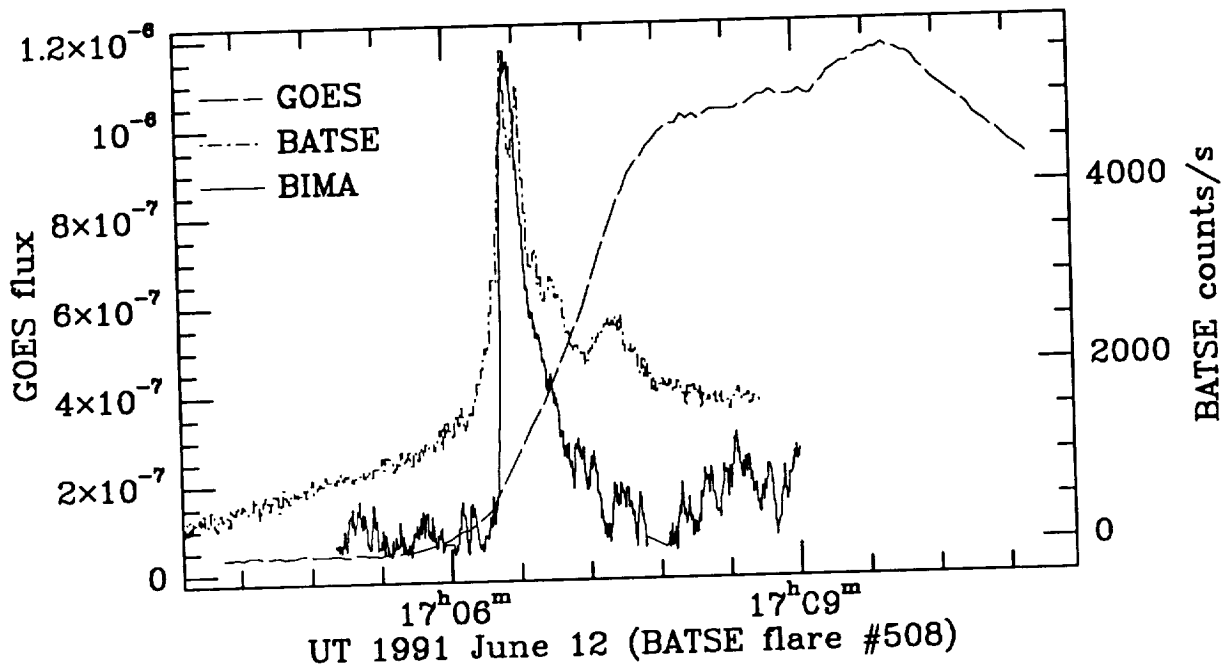
Figure 7 The soft X-ray, hard X-ray and 86 GHz time profiles of a flare at 17 UT on June 12.

Figures 6 and 7 show two examples of flares in which the 86 GHz emission and 25–50 keV hard X-ray emission in the impulsive phase match each other in general terms. We also show the GOES soft-X-ray profiles. Both flares occurred on 1991 June 12; note that the 17 UT flare (Fig. 7) occurred as GRO was emerging from spacecraft-night, which is why the flux is rising so sharply prior to the flare. In both cases the 86 GHz and hard X-ray emissions have impulsive peaks, and there seems to be a delay of the 86 GHz emission with respect to the hard X-ray peak by a few seconds; note, however, that not all hard X-ray peaks are observed in the mm data, as we also noted in the June 13 event discussed above. In these two events the GOES soft X-ray emission does not show any significant rise prior to the onset of 25 – 50 keV emission: it starts near the start of mm/hard X-ray emission, rises slowly and reaches a broad peak after 4-5 minutes and then decays even more slowly, as is normally the case.

Figures 8 and 9 show two cases of events in which impulsive 25 – 50 keV emission was seen, but there was little or no impulsive-phase emission at 86 GHz, even though the count rates at 25 – 50 keV were well above the levels of some small events which produced both 25 – 50 keV and 86 GHz impulsive-phase emission (e.g., Figure 10). The 86 GHz profile in each case shows gradual mm burst emission corresponding roughly with the GOES soft X-ray emission, although the BATSE data show sharp peaks. In one case (Fig. 9) the hard X-ray rise corresponds to the rise phase of both mm and soft X-ray emission; in the second case (Fig. 8), there are two hard X-ray peaks, one of which is located near the start of the GOES and 86 GHz profiles and the other near the peak of the mm emission and corresponding well with a "shoulder" in the GOES profile.
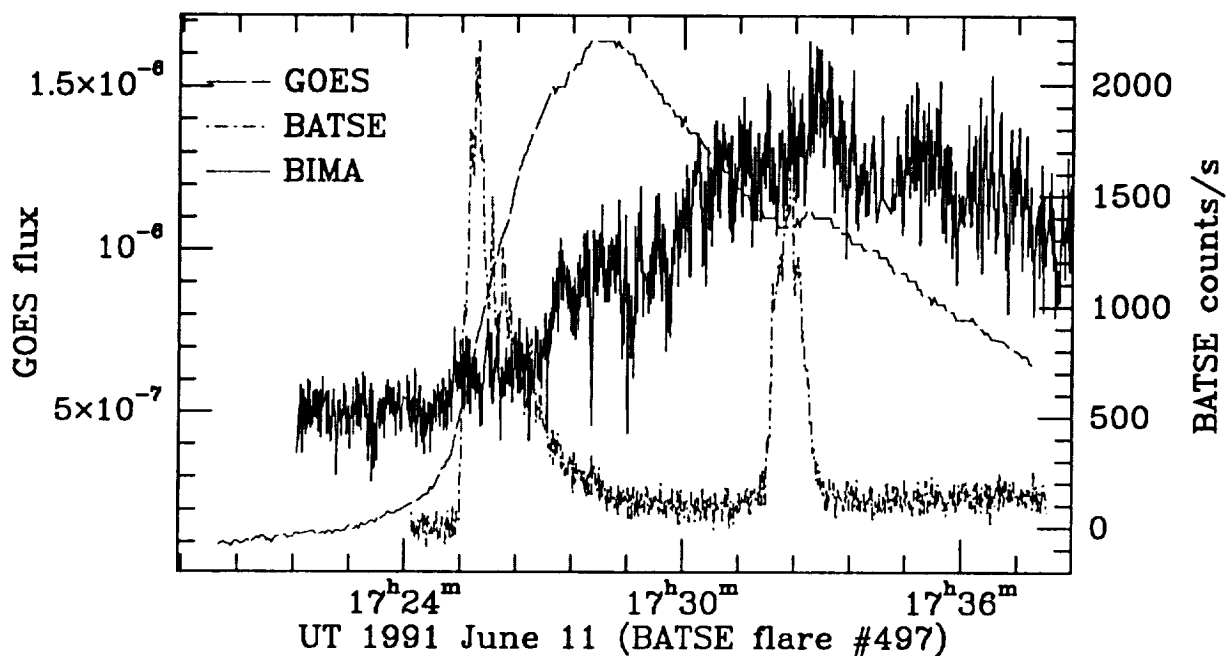
Figure 8 The soft X-ray, hard X-ray and 86 GHz time profiles of a flare at 17:24 UT on June 11. This flare shows impulsive hard X-ray behaviour but no corresponding 86 GHz impulsive phase; instead, an extended thermal phase is seen at 86 GHz.

The final example (Figure 10) is a small event which demonstrates that for simple impulsive events with a very sharp rise, like this one, we see a clear delay of several seconds between the 25 – 50 keV impulsive rise and the 86 GHz rise. In small events such as this there are no counts in the higher-energy BATSE detectors, so we cannot discuss the hard-X-ray spectrum. However, based on earlier discussion we can associate the 86 GHz emission with high-energy electrons (> 300 keV), and the implication is that there is a delay between the production of the 25 – 50 keV electrons and the > 300 keV electrons. Such delays can be attributed to the need to accelerate electrons from low to high energies, and can be used to constrain candidate emission mechanisms. Note also that in this event, unlike some others, the soft X-rays begin to rise well before the hard X-ray onset.

Discussion

Before we discuss our preliminary results, it is useful to consider a basic flare model. There are many flare models in the literature. For the present purpose it is enough to consider a model in which energy release takes place in the corona, resulting in the acceleration of nonthermal electrons. These propagate down magnetic field lines, strike the chromosphere, and produce hard X-rays by thick target bremsstrahlung. The nonthermal electrons deposit ther energy in the chromosphere as heat. The heated, dense chromospheric material produces the flare Hα
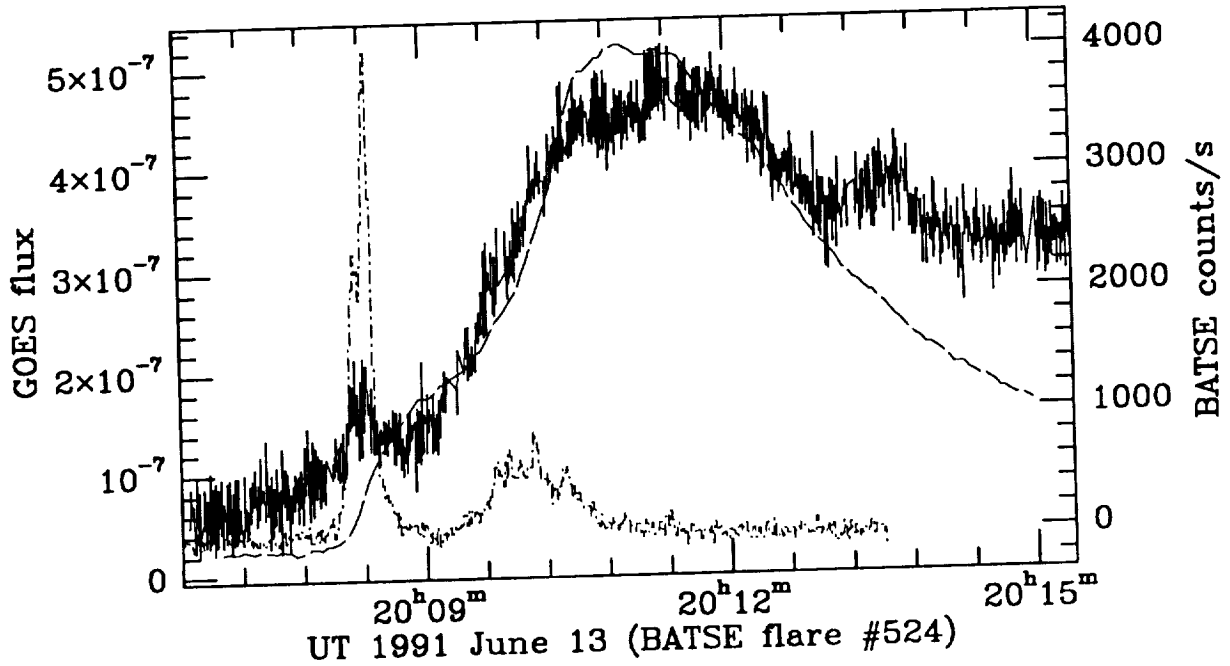
Figure 9 The soft X-ray, hard X-ray and 86 GHz time profiles of a flare at 20 UT on June 13. In this case the 86 GHz emission shows a faint enhancement at the time of the 25 – 50 keV impulsive phase, but is dominated by the thermal decay phase.

emission and rises up into the corona, filling magnetic loops, expanding and producing soft X-rays. Soft X-ray observations show large scale loops at temperatures of millions to several tens of millions of K, covering a much larger area than the original footpoints where nonthermal energy was deposited. There is also soft X-ray emission associated with the preflare phase which indicates the presence of preflare heating, and which often seems to merge smoothly in time with the decay-phase soft X-ray emission.

With these observations we have clearly demonstrated that the millimeter emission provides diagnostics of both the most energetic electrons in solar flares as well as of the thermal decay phase. It does not always bear a close relationship with the 10 – 100 keV electrons. We have shown that there are clear delays between those electrons and the production of the higher energy electrons which radiate at millimeter wavelengths in the impulsive phase.

Thus with the millimeter observations combined with GRO hard X-ray/γ-ray data we will be able to address many problems central to flare physics:

(i) acceleration: The mechanism by which MeV electrons are accelerated is not understood. For example, do the MeV electrons arise naturally as part of the production of 10 – 100 keV electrons, or are they a secondary effect? One type of evidence that GRO will provide will be spectral breaks in the hard X-ray observations, where a different acceleration mechanism takes over. The complementary information provided by BIMA is a more sensitive diagnostic of the numbers of MeV electrons present, and when they are present.
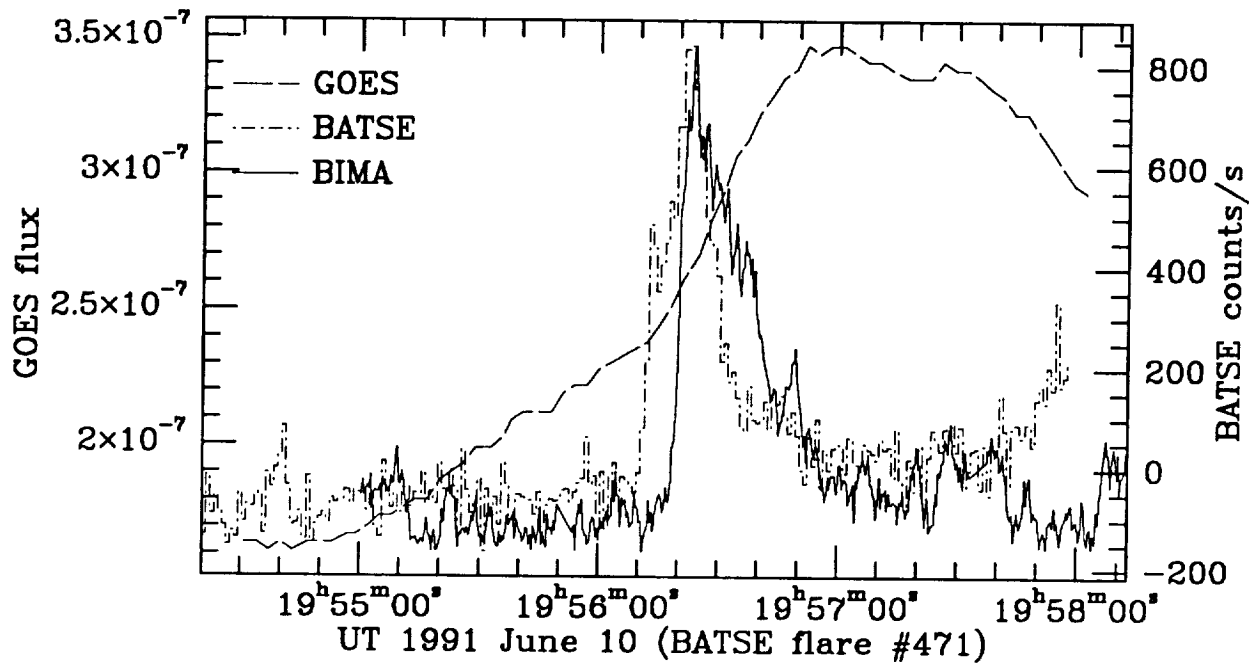
511

C-7

Figure 10 The soft X-ray, hard X-ray and 86 GHz time profiles of a flare at 20 UT on June 10. This small event was not given a GOES classification, and was barely noticeable in the usual log plots of soft-X-ray data. It shows a clear delay between the 86 GHz and hard X-ray profiles; the soft X-ray flux begins to rise well before the onset phase in hard X-rays.

The relationship of the MeV and keV electrons has been studied with SMM-GRS data, but we don't think the picture is at all clear. Millimeter observations give us a larger sample of flares to study than straight gamma-ray data; we can get a good estimate of the high-energy spectral index from radio data alone, and compare it with the lower-energy index derived from GRO data. This will allow us to study

(ii) delays, lifetimes: delays between BIMA (MeV electrons) and hard X-ray-emitting (25–50 keV) electrons will be important, since they can be interpreted as the time needed to accelerate electrons from 50 keV to 1 MeV, and thus can be compared with predictions of various models.

(iii) locations, source sizes: millimeter observations will provide images of the MeV electrons as long as they are in magnetic fields. The electrons might not strike the chromosphere at the footpoints of loops with strong fields because of magnetic mirroring. Do gamma ray-emitting electrons just occupy one loop or do they occupy several loops? Do γ-rays come from electrons precipitating in weak-field regions? This may require diffusion of electrons across field lines, usually a slow process. Are wave particle interactions needed to play a role?

Conclusions

Our 1991 June observations permit us to arrive at the following tentative conclusions.

512

1) There are two phases in millimeter burst emission: a nonthermal impulsive phase and a thermal gradual phase. Both phases are often observed in the same flare.

2) Impulsive-phase millimeter burst emission probes MeV electrons produced during flares. Some flares show no nonthermal impulsive phase at millimeter wavelengths, although they seem to show it at 25–50 keV electrons. These gradual phase flares correspond well to the GOES soft X-ray emission.

3) Even in flares which do show impulsive phase millimeter emission, correlation of the mm emission with electrons of 25 – 100 keV is often poor.

4) Millimeter emission usually occurs at the steep rise phase of the hard X-ray emitting electrons (25–100 keV). There appears to exist some delay between BIMA mm-emission onset and BATSE 25–100 keV X-ray data. Both results have implications in the particle acceleration process.

In 1992 the BIMA array will begin to operate with 6 dishes, providing 15 baselines. This will allow us to map the sources of 86 GHz emission in the impulsive phase of flares, and this should tell us a great deal about the spatial distribution and origin of the gamma-ray emitting electrons.

Acknowledgements

Bibliography

Kaufmann, P., Correia, E., Costa, J. E. R., Vaz, A. M. Z., & Dennis, B. R. 1985, *Nat*, **313**, 380.

Kundu, M. R., White, S. M., Gopalswamy, N., Bieging, J. H., & Hurford, G. J. 1990, *ApJL*, **358**, L69.

Ramaty, R. 1969, *ApJ*, **158**, 753.

Ramaty, R., & Petrosian, V. 1972, *ApJ*, **178**, 241.

White, S. M., & Kundu, M. R. 1992, *Solar Phys.*, in preparation.